Iranian Journal of Analytical Chemistry
Volume 8, Issue 2, September 2021 (80-89) Origonal Research Article

مجله ایرانی شیمی تجزیه
دوره۸، شماره ۲، مهرماه ۱۴۰۰ (۸۹-۸۰)

Hybridization of Phosphomolybdic Acid with Hexamine and Hexamine-Nickel for Improving of Activity in Photodegradation of Dyes Under Sunlight Irradiation

Mehdi Taghdiri[1, 2, *], Farzaneh Ghanei[1], Marzieh Ardakani[1], Seyed Hossein Banitaba[1,2], Hossein Aarabi Ardakani[1]
1. Department of Chemistry, Payame Noor University, 19395-3697 Tehran, Iran
2. Research Center of Environmental Chemistry, Payame Noor University, Ardakan, Yazd, Iran
Received: 17 August 2021 **Accepted:** 21 September 2021
DOI: 10.30473/ijac.2022.62496.1219

Abstract
Two new organic hybrids of phosphomolybdic acid (PMA) were prepared by means of hexamine (HMT) and HMT-Ni^{2+} complex. The effects of hybridization of HMT and Ni^{2+} were investigated on the photocatalytic activity of PMA. Characterization of hybrids were carried out by elemental analyses, Fourier transform infrared spectroscopy, powder X-ray diffraction, thermogravimetric analysis and differential scanning calorimetry. The band gaps of PMA, phosphomolybdate-hexamine (PMA-HMT) and phosphomolybdate-hexamine-nickel (PMA-HMT-Ni) were determined from the diffuse reflectance spectra using the Tauc plots. Dye adsorption and photocatalytic properties of PMA-HMT and PMA-HMT-Ni hybrids were examined by studying the decolorization of model dyes methylene blue (MB), rhodamine B (RhB) and mixtures of MB and methyl orange (MO) solutions. The results show that the band gap of PMA-HMT-Ni is narrower and hence, its photocatalytic activity is higher for the degradation of dyes under sunlight irradiation. Mechanism of photodegradation was studied by adding scavengers. Removal is via combination of adsorption and then photocatalytic degradation through oxidation by radicals.

Keywords
Photocatalyst; Polyoxometalate; Dyes, Band Gap; Organic-Inorganic Hybrid, Solar Light.

1. INTRODUCTION

Engineering of the electronic band gap of materials has recently become the focus of attention to shift the band gap toward visible region for application in solar cells [1], semiconducting devices [2], enhanced optoelectronics [3] and visible-light photocatalysis [4]. Various approaches have been used for band gap narrowing e.g. heteroatom doping, self-doping, interface engineering (Heterojunction), dye-sensitization and prediction by density functional theory (DFT) and its local density approximation (LDA) [4]. The importance of this emerging field leaded us to evaluate variation of optical band gap of semiconductor-like polyoxometalates (POMs) upon hybridization with organic or organometallic moieties so that POMs could be utilized for solar light (or visible light) photocatalysis. POMs i.e. the anions of heteropoly acids are clusters of transition metal oxyanions with shared oxygen atoms. Such three-dimensional frameworks exhibit attractive properties such as high reactivity, excellent stability, stronger acidity than conventional inorganic acids, fast reversible redox transformations and high photocatalytic and oxidizing activity. Practically, photo-excitation of POMs needs the ultraviolet (UV) light that includes 4–5% of solar radiation and hence the application of lone POMs is uneconomical. Consequently, efficiency of POMs is poor in the visible region of the solar spectrum due to their wide band gaps [5, 6]. The design of novel organic-inorganic hybrids due to incorporating organic ligands onto the POM platform not only allows the tuning of the relatively wide band gap of POMs but also overcomes the major drawback of high solubility of lone POMs in water and polar solvents [7-10].

In this regard, we represent tow new hybrid compounds containing phosphomolybdic acid (PMA, $H_3PMo_{12}O_{40}$), hexamine or hexamethylenetetramine (HMT), an easily available, very cheap and nontoxic amine and or Ni^{2+} as the transition metal linker.

2. EXPERIMENTAL

2.1. Chemicals and reagents

Phosphomolybdic acid, NaOH (99%), HCl (aqueous solution, 37 wt. %), $Ni(NO_3)_2.6H_2O$, Isopropyl alcohol (99%), benzoquinone and KI were purchased from Merck. The hexamethylenetetramine (HMT) or hexamine powder ($C_6H_{12}N_4$, 99.5%) was from Sina Chemical Industries Co. (Shiraz, Iran). Other reagents were purchased from commercial sources, and used without further purification.

*Corresponding Author: mehditaghdiri@yahoo.com

2.2. Apparatus

Weighing of materials was performed using an analytical balance model Sartorius MCBA 100 with precision of ±0.0001 g. A Labinco magnetic stirrer model L-81 was used for stirring of solutions. For pH measurements, a Metrohm type 691 pH-meter was used. A GBC UV-Vis spectrophotometer model Cintra 6 was used for spectrophotometric measurements. The IR spectra were obtained with KBr pellets using a Shimadzu 8400s FTIR spectrometer. X-ray diffraction patterns were carried out on a Bruker D8 advance X-ray diffractometer using Cu target at room temperature. C, H and N elemental analyses were carried out on Perkin-Elmer 2400 CHN elemental analyzer. Solid state diffuse reflectance spectrum (DRS) was recorded on an Avantes spectrometer (AvaSpec-2048-TEC), using $BaSO_4$ as a standard. The thermogravimetric analysis (TGA) and differential scanning calorimetry (DSC) was performed on a Rheometric Scientific STA 1500 thermal analyzer under the atmosphere of air.

2.3. Preparation of organic-inorganic hybrids

PMA-HMT hybrid was prepared as following: 10 mL aqueous solution of HMT (1.0 % w/w) was added to 10 mL aqueous solution of PMA (7.5 % w/w). A yellow suspension solution was produced immediately. The mixture was stirred at 500 rpm by a magnetic agitator at ambient temperature for 3 h. The suspension was separated and the collected solid was washed with distilled water and then dried at 100 °C. A green solid was obtained. For PMA-HMT-Ni, 5 mL ethanolic solution of HMT (2.0 % w/w) was added to 5 mL aqueous solution of $Ni(NO_3)_2.6H_2O$ (4.0 % w/w). Then, 5 mL ethanolic solution of PMA (13.0 % w/w) was added to the mixture of HMT and Ni^{2+}. A yellow suspension solution was produced immediately and after providing similar process with PMA-HMT, green solid was obtained.

2.4. Photocatalytic activity for degradation of dyes

MB and RhB solutions with definite concentrations were prepared. The pH of the solutions was adjusted on the desired values by adding dilute HCl and NaOH solutions. The dye solutions and predetermined amount of hybrids were moved to a beaker, capped by cellophane and exposed to sunlight. After a particular reaction time, absorbance of the dye solutions was determined. It is noteworthy that the sunlight exposure tests were performed on October 2017 in Payame Noor University, Ardakan, Yazd, Iran (GPS coordinates: N = 32° 29′, E=53° 59′). The solar radiation intensity in Yazd province is about 800 W/m^2 in summer [11]. It should be noted, the solutions were not stirred during solar irradiation. The C/C_0 values were obtained through the maximum absorption in the whole absorption spectrum in order to plot C/C_0 vs. time curves.

2.5. Kinetic analysis

The kinetic analysis of decolorization was carried out using the pseudo-first-order kinetics, $\ln(A_0/A_t)=\ln(C_0/C_t)=kt$, where A_0 and C_0 is the initial absorbance and concentration of dye solution; A_t and C_t is the absorbance and concentration of dye solution at time t, and the slope k is the kinetic constant in min^{-1}. All C_0/C_t values were obtained through the maximum absorption in the whole absorption spectrum in order to plot $\ln(C_0/C_t)$ vs. t.

3. RESULT AND DISCUSSION

3.1. Characterizations of hybrids

The FTIR spectra of HMT, PMA, PMA-HMT and PMA-HMT-Ni are shown in Fig. 1a. The IR spectra of PMA-HMT and PMA-HMT-Ni exhibit the characteristic bands of the HMT organic moieties and of PMA inorganic moieties. The strong absorption peaks at 1100-750 cm^{-1} show the presence of $PMo_{12}O_{40}^{3-}$ anions with α-Keggin structure. The band of about 880 cm^{-1} is related to the Mo-O_b-Mo stretching mode of PMA while the band of about 970 cm^{-1} corresponds to its Mo-O_d scissoring mode. Nevertheless, the FTIR spectrum of PMA-HMT-Ni showed significant differences in 1300-1500 cm^{-1} in comparison with PMA-HMT that it can be attributed to coordination of HMT to the metal ion [12].

The band at 1389 cm^{-1} has been assigned to uncoordinated NO_3^- ion [13].

The 3238 and 1418 cm^{-1} peaks in the FTIR spectrum of PMA-HMT are indicative the presence of ammonium ions in the hybrid structure because these peaks correspond to the N–H bonds in NH_4^+ [14, 15].

The XRD patterns of HMT, PMA, PMA-HMT and PMA-HMT-Ni are depicted in Fig. 1b. It is clear that the PMA-HMT and PMA-HMT-Ni precursors contain HMT and PMA. In hybrids, the positions of the sharp peaks below 2θ = 15° can be ascribed to $PMo_{12}O_{40}^{3-}$. Therefore, the primary structure of POM has remained intact in the solid structure of hybrids. There is a new peak at 2θ = 11.85° in PMA-HMT and PMA-HMT-Ni hybrids unlike PMA and HMT primers. On the other hand, the existence of similar peak in ammonium phosphomolybdate [14] can be evidence for the presence of attached ammonium ions to PMA in the hybrids. The XRD of PMA-HMT-Ni demonstrate difference at peak about 2θ = 7° in comparison with PMA and PMA-HMT. The presence of this peak is indicative of complex formation between Ni^{2+} and HMT [12].

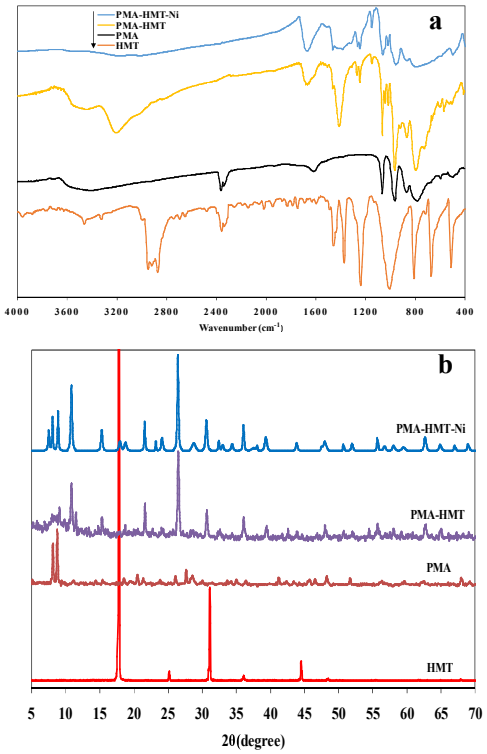

Fig. 1. (a) FTIR spectra of HMT, PMA, PMA-HMT and PMA-HMT-Ni, (b) X-ray diffraction patterns of HMT, PMA and PMA-HMT-Ni.

The band gaps of PMA, PMA-HMT and PMA-HMT-Ni were determined from the diffuse reflectance spectrum (Fig. 2a) using the Tauc's plot (Fig. 2b). The band gap of PMA decreased due to hybridization (Table 1). The calculated band gap of PMA (2.86 eV) is compatible with the values reported in the literature [16-18]. With the adding of HMT into the PMA structure, the band gap decreased to 2.45 eV in PMA-HMT. With the incorporation of Ni into the PMA-HMT, the band gap decreased further down to 2.18 eV in PMA-HMT-Ni. The band gap has been shifted from preliminary visible region (433 nm) into middle visible region (569 nm).

The stoichiometric formula of $[C_6H_{13}N_4]_{15}[(NH_4)PMo_{12}O_{40}]_6[(NH_4)_2PMo_{12}O_{40}]_3.43H_2O$ was suggested for PMA-HMT from the carbon, hydrogen and nitrogen elemental analyses (C, 5.47%; H, 1.45%; N, 5.15%) and the presence of ammonium groups based on the FTIR and XRD interpretation. On the basis of this composition, the calculated elemental analyses are: C, 5.54%; H, 1.45%; N, 5.17%. The similar method suggested the stoichiometric formula of $Ni_7[C_6H_{12}N_4]_{14}[(NH_4)PMo_{12}O_{40}]_4[(NH_4)_2PMo_{12}O_{40}]_4(NO_3)_2.24H_2O$ for PMA-HMT-Ni. The elemental analyses (C, 5.80%; H, 1.50%; N, 5.50%) are in good agreement with the proposed formula (C, 5.69%; H, 1.50%; N, 5.53%).

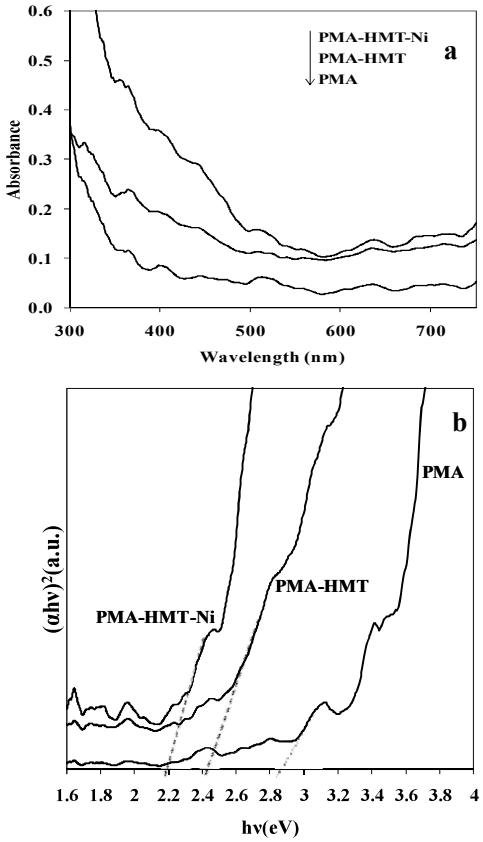

Fig. 2. DRS spectra (a) and Tauc's plots (b) of PMA, PMA-HMT and PMA-HMT-Ni.

Table 1. Optical band gap and exciting wavelength of PMA, PMA-HMT and PMA-HMT-Ni

Sample	Band gap (eV)	λ (nm)
PMA	2.86	433
PMA-HMT	2.45	506
PMA-HMT-Ni	2.18	569

The TG and DSC curves of PMA-HMT and PMA-HMT-Ni hybrids are shown in Fig. 3. In the TG curve of PMA-HMT, the initial weight loss of 7.27% at 265 °C is ascribed to the loss of coordinated water molecules, three HMT molecules attached to $(NH_4)_2PMo_{12}O_{40}^-$ and ammonium ions (the calculated value is 7.25%). The second weight loss of 8.24% from 265 to 479 °C is ascribed to the loss of the strong binding HMT molecules (i.e. twelve hexamine molecules attached to $(NH_4)PMo_{12}O_{40}^{2-}$). The calculated value is 8.68%. The whole weight loss of 15.51% is in accordance with the hybrid composition (calculated value = 15.93%). The same steps are observed for the TG curve of PMA-HMT-Ni (Fig. 3b). The initial weight loss of 7.55% at 285 °C is related to the loss of water molecules, four weak binding HMT molecules, ammonium and nitrate ions (the calculated value is 7.52%). The second weight loss of 7.80% from 285 to 474 °C is from

the strong binding HMT molecules (the calculated value is 7.91%). The calculated value of 15.43% based on proposed PMA-HMT-Ni composition is consistent with obtained whole weight loss of 15.35%. The residual products are MoO_3 and P_2O_5 [14]. Besides, the NiO is produced from the decomposition of PMA-HMT-Ni [19]. Also, the DSC curves show similar behavior. The first and second peaks at ca. 260 °C and 320 °C correspond to release of ammonia from decomposition of ammonium phosphomolybdate [15, 20] and the decomposition of HMT molecules to formaldehyde and ammonia [21]. It should be noted that the decomposition of HMT is very complicated and includes endothermic and dominant exothermic peaks at ca. 260 °C [22, 23]. The oxidation of evolved NH_3 at ca. 470 °C with air under the catalytic effect of formed oxides creates the bifurcate peaks [24]. The obtained peaks at about 780 °C are the melting point of the produced oxides [24].

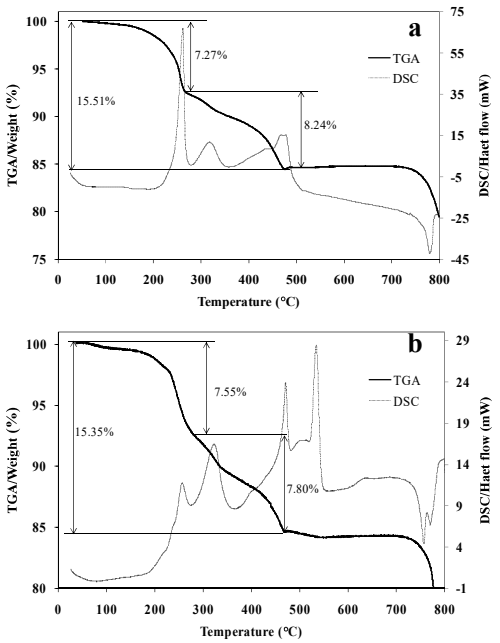

Fig. 3. TGA and DSC curves of PMA-HMT (a) and PMA-HMT-Ni (b).

3.2. Hybrids activity for removal and degradation of dyes

3.2.1. Photocatalytic degradation of MB

At first, the efficiency of hybrids was evaluated by removal and degradation of MB. Before the photocatalytic degradation, adsorption of MB on the hybrids was evaluated. The hybrids were then tested as catalyst for the photocatalytic degradation of MB. Results (Fig. 4) show that photocatalytic degradation displays higher kinetic and removal efficiency than adsorption. Moreover, the higher kinetic and removal efficiency of PMA-HMT-Ni hybrid is evident in comparison with PMA-HMT hybrid. The kinetic and removal efficiency of MB in the solar photocatalytic process with PMA-HMT-Ni are 0.0519 min^{-1} and 98.4 % respectively, whilst these are 0.0124 min^{-1} and 82.6 % with PMA-HMT hybrid (Fig. 4c, d).

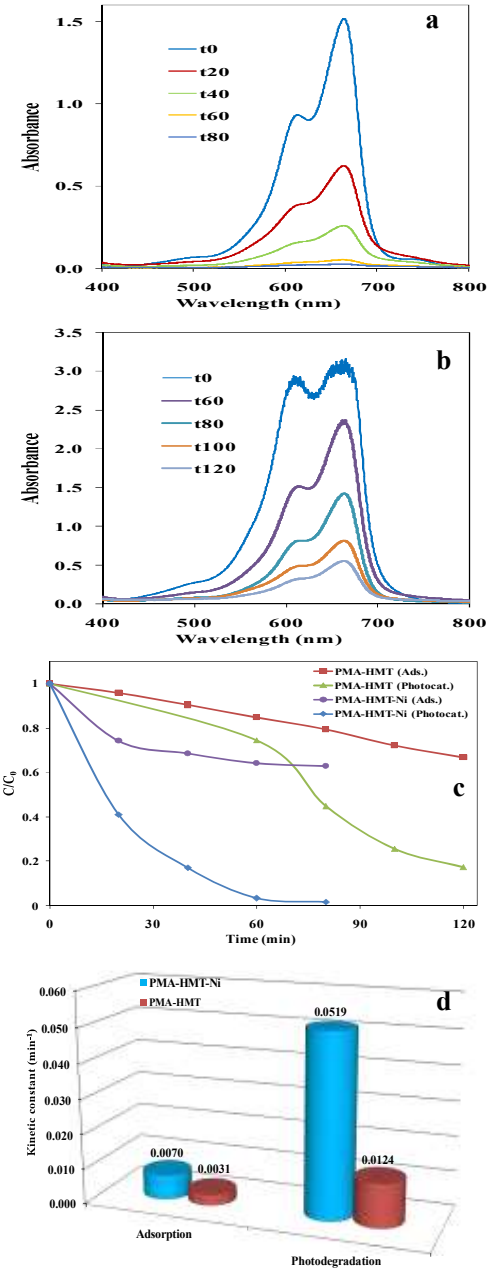

Fig. 4. UV-Vis absorption spectra of the MB solution during the photodegradation under sunlight in the presence of the PMA-HMT-Ni (a) and PMA-HMT (b), C/C_0 vs. time for a, b and during adsorption on the PMA-HMT-Ni and the PMA-HMT (c) and the kinetic constants (d).

3.2.2. Photocatalytic degradation of RhB

The PMA-HMT-Ni was applied for photodecomposition of RhB under sunlight irradiation due to more photocatalytic activity. UV-Vis absorption spectra of RhB (15 mg/L, 100 mL, pH=1.5) during the photodegradation under sunlight without photocatalyst (photolysis), during the adsorption and photodegradation under sunlight in the presence of the PMA-HMT-Ni have been shown in Fig. 5a-c. The photodegradation of RhB is negligible due to photolysis (Fig. 5a). PMA-HMT-Ni adsorbs RhB because RhB (pKa=3.1) is as cationic form in pH 1.5 (Fig. 5b). The sunlight accelerates the removal of RhB in the presence of PMA-HMT-Ni (0.1 g/L) (Fig. 5c).

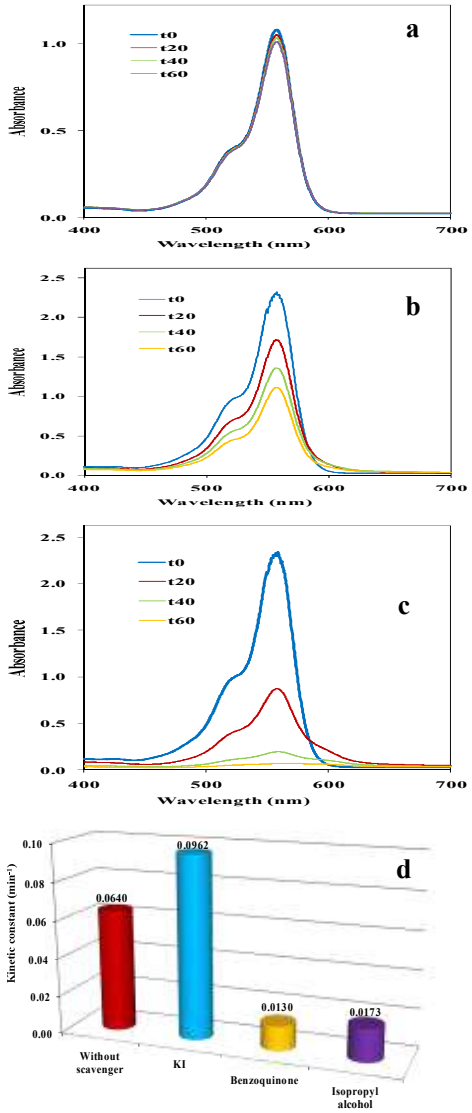

Fig. 5. UV-Vis absorption spectra of the RhB solution during the photodegradation under sunlight (a), during the adsorption in the dark on the PMA-HMT-Ni (b), during the photodegradation under sunlight in the presence of the PMA-HMT-Ni (c) and the kinetic constants in the presence of scavengers (d).

3.2.3. Adsorption and photocatalytic activity for mixture of MB and MO

In order to study the ability of hybrid for degradation of mixed dye solution, the mixture of MB and MO was prepared and used. Fig. 6 shows the experiments results of the mixed solution of MB and MO in the presence of 0.5 g/L of PMA-HMT in the pH 7.0. Fig. 6a shows the spectra of the mixed solutions of MB and MO during the photodegradation under solar light irradiation and clearly confirms that PMA-HMT degrades both MB and MO dyes. Besides, the PMA-HMT adsorbs not only MB but also MO, even though MO is as anionic form in the pH 7.0 (Fig. 6b). The PMA-HMT has a surface negative charge. Hence, the cationic MB molecules are preferentially adsorbed on it. Then, the surface of the hybrid possessing a slightly positive charge adsorbs the anionic MO molecules. Indeed, the degradation of MO is due to its adsorption (Fig. 6b).

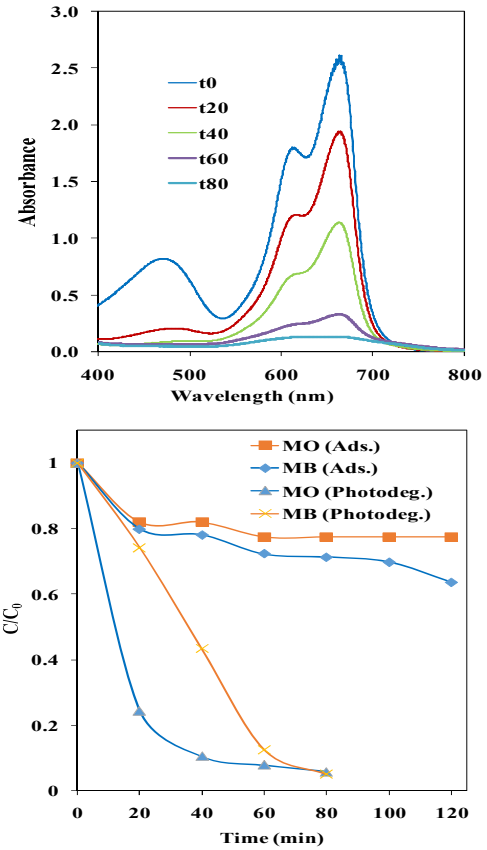

Fig. 6. UV-Vis absorption spectra of the 20 mL mixed solution of MO (10 mg/L) and MB (15 mg/L) during the photodegradation under sunlight in the presence of the PMA-HMT (a) and C/C_0 vs. time for a and during adsorption (b).

3.3. Mechanism of photodegradation

As it was seen, the photodegradation of MO in the mixed solution with MB (Fig. 6) is due to uptake

of it on the surface of the hybrid after uptake of MB. Therefore, the photodegradation mechanism takes place through dye-sensitized degradation. Dye-sensitized degradations take place in cases where there exists an interaction between dye and photocatalyst [25].

A photodegradation mechanism can be proposed according to following steps:

1) Photoexcitation: irradiation of the hybrid with light (*hv*) results in the formation of the excited state ([PMA-HMT]*or PMA-HMT-Ni]*) without significant change on its molecular structure:

$$\text{hybrid} + hv \rightarrow [\text{hybrid}]^* \quad (1)$$

2) Oxidation of organic compound: the [hybrid]* is a strong oxidant able to oxidize and, most often, mineralize organic dyes. The excited hybrid is reduced with excited organic dye in aqueous solution through reactions 2-4,

$$\text{Dye} + hv \rightarrow \text{Dye}^* \quad (2)$$

$$[\text{hybrid}]^* + \text{Dye}^* \rightarrow [\text{hybrid}](e^-) + \text{Dye}^{+\bullet} \quad (3)$$

$$\text{Dye}^{+\bullet} \rightarrow\cdots\rightarrow \text{decomposition into colorless products} \quad (4)$$

3) Reoxidation of reduced hybrid: the [hybrid](e^-) is re-oxidized by bulk dioxygen which undergoes reductive activation through the formation of $O_2^{\bullet-}$ or $^{\bullet}OH$ radicals,

$$[\text{hybrid}](e^-) + O_2 \rightarrow [\text{hybrid}] + O_2^{\bullet-} \quad (5)$$

$$O_2^{\bullet-} + H^+ \rightarrow\cdots\rightarrow {}^{\bullet}OH \quad (6)$$

4) Oxidation of organic dye by produced radicals:

$$\text{Dye} + O_2^{\bullet-} \text{ or } {}^{\bullet}OH \rightarrow \text{oxidized products} \quad (7)$$

The decrease of the decolorization rate in the presence of isopropyl alcohol, as scavenger of $^{\bullet}OH$, and benzoquinone, as scavenger of $O_2^{\bullet-}$, confirm the role of hydroxyl and superoxide radicals in the degradation of dye (Fig. 5d). The increase of the decolorization rate in the presence of potassium iodide, as scavenger of h^+, indicates the hole does not play role in the degradation of dye (Fig. 5d).

4. CONCLUSION

3.1. Characterizations of hybrids

The FTIR spectra of HMT, PMA, PMA-HMT and PMA-HMT-Ni are shown in Fig. 1a. The IR spectra of PMA-HMT and PMA-HMT-Ni exhibit the characteristic bands of the HMT organic moieties and of PMA inorganic moieties. The strong absorption peaks at 1100-750 cm^{-1} show the presence of $PMo_{12}O_{40}^{3-}$ anions with α-Keggin structure. The band of about 880 cm^{-1} is related to the Mo-O_b-Mo stretching mode of PMA while the band of about 970 cm^{-1} corresponds to its Mo-O_d scissoring mode. Nevertheless, the FTIR spectrum of PMA-HMT-Ni showed significant differences in 1300-1500 cm^{-1} in comparison with PMA-HMT that it can be attributed to coordination of HMT to the metal ion [12]. The band at 1389 cm^{-1} has been assigned to uncoordinated NO_3^- ion [13]. The 3238 and 1418 cm^{-1} peaks in the FTIR spectrum of PMA-HMT are indicative the presence of ammonium ions in the hybrid structure because these peaks correspond to the N–H bonds in NH_4^+ [14, 15].

The XRD patterns of HMT, PMA, PMA-HMT and PMA-HMT-Ni are depicted in Figure 1b. It is clear that the PMA-HMT and PMA-HMT-Ni precursors contain HMT and PMA. In hybrids, the positions of the sharp peaks below 2θ = 15° can be ascribed to $PMo_{12}O_{40}^{3-}$. Therefore, the primary structure of POM has remained intact in the solid structure of hybrids. There is a new peak at 2θ = 11.85° in PMA-HMT and PMA-HMT-Ni hybrids unlike PMA and HMT primers. On the other hand, the existence of similar peak in ammonium phosphomolybdate [14] can be evidence for the presence of attached ammonium ions to PMA in the hybrids. The XRD of PMA-HMT-Ni demonstrate difference at peak about 2θ = 7° in comparison with PMA and PMA-HMT. The presence of this peak is indicative of complex formation between Ni^{2+} and HMT [12].

The band gaps of PMA, PMA-HMT and PMA-HMT-Ni were determined from the diffuse reflectance spectrum (Figure 2a) using the Tauc's plot (Figure 2b). The band gap of PMA decreased due to hybridization (Table 1). The calculated band gap of PMA (2.86 eV) is compatible with the values reported in the literature [16-18]. With the adding of HMT into the PMA structure, the band gap decreased to 2.45 eV in PMA-HMT. With the incorporation of Ni into the PMA-HMT, the band gap decreased further down to 2.18 eV in PMA-HMT-Ni. The band gap has been shifted from preliminary visible region (433 nm) into middle visible region (569 nm).

The stoichiometric formula of $[C_6H_{13}N_4]_{15}[(NH_4)PMo_{12}O_{40}]_6[(NH_4)_2PMo_{12}O_{40}]_3.43H_2O$ was suggested for PMA-HMT from the carbon, hydrogen and nitrogen elemental analyses (C, 5.47%; H, 1.45%; N, 5.15%) and the presence of ammonium groups based on the FTIR and XRD interpretation. On the basis of this composition, the calculated elemental analyses are: C, 5.54%; H, 1.45%; N, 5.17%. The similar method suggested the stoichiometric formula of $Ni_7[C_6H_{12}N_4]_{14}[(NH_4)PMo_{12}O_{40}]_4[(NH_4)_2PMo_{12}O_{40}]_4(NO_3)_2.24H_2O$ for PMA-HMT-Ni. The elemental analyses (C, 5.80%; H, 1.50%; N, 5.50%) are in good agreement with the proposed formula (C, 5.69%; H, 1.50%; N, 5.53%).

The TG and DSC curves of PMA-HMT and PMA-HMT-Ni hybrids are shown in Figure 3. In the TG curve of PMA-HMT, the initial weight loss of 7.27% at 265 °C is ascribed to the loss of coordinated water molecules, three HMT molecules attached to $(NH_4)_2PMo_{12}O_{40}^-$ and

ammonium ions (the calculated value is 7.25%). The second weight loss of 8.24% from 265 to 479 °C is ascribed to the loss of the strong binding HMT molecules (i.e. twelve hexamine molecules attached to $(NH_4)PMo_{12}O_{40}^{2-}$). The calculated value is 8.68%. The whole weight loss of 15.51% is in accordance with the hybrid composition (calculated value = 15.93%). The same steps are observed for the TG curve of PMA-HMT-Ni (Figure 3b). The initial weight loss of 7.55% at 285 °C is related to the loss of water molecules, four weak binding HMT molecules, ammonium and nitrate ions (the calculated value is 7.52%). The second weight loss of 7.80% from 285 to 474 °C is from the strong binding HMT molecules (the calculated value is 7.91%). The calculated value of 15.43% based on proposed PMA-HMT-Ni composition is consistent with obtained whole weight loss of 15.35%. The residual products are MoO_3 and P_2O_5 [14]. Besides, the NiO is produced from the decomposition of PMA-HMT-Ni [19]. Also, the DSC curves show similar behavior. The first and second peaks at ca. 260 °C and 320 °C correspond to release of ammonia from decomposition of ammonium phosphomolybdate [15, 20] and the decomposition of HMT molecules to formaldehyde and ammonia [21]. It should be noted that the decomposition of HMT is very complicated and includes endothermic and dominant exothermic peaks at ca. 260 °C [22, 23]. The oxidation of evolved NH_3 at ca. 470 °C with air under the catalytic effect of formed oxides creates the bifurcate peaks [24]. The obtained peaks at about 780 °C are the melting point of the produced oxides [24].

3.2. Hybrids activity for removal and degradation of dyes

3.2.1. Photocatalytic degradation of MB

At first, the efficiency of hybrids was evaluated by removal and degradation of MB. Before the photocatalytic degradation, adsorption of MB on the hybrids was evaluated. The hybrids were then tested as catalyst for the photocatalytic degradation of MB. Results (Figure 4) show that photocatalytic degradation displays higher kinetic and removal efficiency than adsorption. Moreover, the higher kinetic and removal efficiency of PMA-HMT-Ni hybrid is evident in comparison with PMA-HMT hybrid. The kinetic and removal efficiency of MB in the solar photocatalytic process with PMA-HMT-Ni are 0.0519 min^{-1} and 98.4 % respectively, whilst these are 0.0124 min^{-1} and 82.6 % with PMA-HMT hybrid (Figure 4c, d).

3.2.2. Photocatalytic degradation of RhB

The PMA-HMT-Ni was applied for photodecomposition of RhB under sunlight irradiation due to more photocatalytic activity. UV-Vis absorption spectra of RhB (15 mg/L, 100 mL, pH=1.5) during the photodegradation under sunlight without photocatalyst (photolysis), during the adsorption and photodegradation under sunlight in the presence of the PMA-HMT-Ni have been shown in Figure 5a-c. The photodegradation of RhB is negligible due to photolysis (Figure 5a). PMA-HMT-Ni adsorbs RhB because RhB (pKa=3.1) is as cationic form in pH 1.5 (Figure 5b). The sunlight accelerates the removal of RhB in the presence of PMA-HMT-Ni (0.1 g/L) (Figure 5c).

3.2.3. Adsorption and photocatalytic activity for mixture of MB and MO

In order to study the ability of hybrid for degradation of mixed dye solution, the mixture of MB and MO was prepared and used. Figure 6 shows the experiments results of the mixed solution of MB and MO in the presence of 0.5 g/L of PMA-HMT in the pH 7.0. Figure 6a shows the spectra of the mixed solutions of MB and MO during the photodegradation under solar light irradiation and clearly confirms that PMA-HMT degrades both MB and MO dyes. Besides, the PMA-HMT adsorbs not only MB but also MO, even though MO is as anionic form in the pH 7.0 (Figure 6b). The PMA-HMT has a surface negative charge. Hence, the cationic MB molecules are preferentially adsorbed on it. Then, the surface of the hybrid possessing a slightly positive charge adsorbs the anionic MO molecules. Indeed, the degradation of MO is due to its adsorption (Figure 6b).

3.3. Mechanism of photodegradation

As it was seen, the photodegradation of MO in the mixed solution with MB (Figure 6) is due to uptake of it on the surface of the hybrid after uptake of MB. Therefore, the photodegradation mechanism takes place through dye-sensitized degradation. Dye-sensitized degradations take place in cases where there exists an interaction between dye and photocatalyst [25].

A photodegradation mechanism can be proposed according to following steps:

1) Photoexcitation: irradiation of the hybrid with light ($h\nu$) results in the formation of the excited state ([PMA-HMT]*or PMA-HMT-Ni]*) without significant change on its molecular structure:

$$\text{hybrid} + h\nu \rightarrow [\text{hybrid}]^* \quad (1)$$

2) Oxidation of organic compound: the [hybrid]* is a strong oxidant able to oxidize and, most often, mineralize organic dyes. The excited hybrid is reduced with excited organic dye in aqueous solution through reactions 2-4,

$$\text{Dye} + h\nu \rightarrow \text{Dye}^* \quad (2)$$

$$[\text{hybrid}]^* + \text{Dye}^* \rightarrow [\text{hybrid}](e^-) + \text{Dye}^{+\bullet} \quad (3)$$

$Dye^{+\bullet} \rightarrow\cdots\rightarrow$ decomposition into colorless products (4)

3) Reoxidation of reduced hybrid: the [hybrid](e^-) is re-oxidized by bulk dioxygen which undergoes reductive activation through the formation of $O_2^{\bullet-}$ or $^{\bullet}OH$ radicals,

[hybrid](e^-) + O_2 → [hybrid] + $O_2^{\bullet-}$ (5)

$O_2^{\bullet-} + H^+ \rightarrow\cdots\rightarrow {}^{\bullet}OH$ (6)

4) Oxidation of organic dye by produced radicals:

Dye + $O_2^{\bullet-}$ or $^{\bullet}OH$ → oxidized products (7)

The decrease of the decolorization rate in the presence of isopropyl alcohol, as scavenger of $^{\bullet}OH$, and benzoquinone, as scavenger of $O_2^{\bullet-}$, confirm the role of hydroxyl and superoxide radicals in the degradation of dye (Figure 5d). The increase of the decolorization rate in the presence of potassium iodide, as scavenger of h^+, indicates the hole does not play role in the degradation of dye (Figure 5d).

REFERENCES

[1] Z. Hu, Z. Lin, J. Su, J. Zhang, J. Chang, Y. Hao, A Review on Energy Band-Gap Engineering for Perovskite Photovoltaics, *Solar RRL*, 3 (2019) 1900304.

[2] W.-J. Su, H.-C. Chang, Y.-T. Shih, Y.-P. Wang, H.-P. Hsu, Y.-S. Huang, K.-Y. Lee, Two dimensional MoS2/graphene pn heterojunction diode: Fabrication and electronic characteristics, *J. Alloys Compd*., 671 (2016) 276-282.

[3] H. Van Mullekom, J. Vekemans, E. Havinga, E. Meijer, Developments in the chemistry and band gap engineering of donor–acceptor substituted conjugated polymers, *Mat. Sci. Eng.: R: Reports*, 32 (2001) 1-40.

[4] R.B. Marcelino, C.C. Amorim, Towards visible-light photocatalysis for environmental applications: band-gap engineering versus photons absorption—a review, *Env . Sci. Poll. Res*, 26 (2019) 4155-4170.

[5] R. Wang, Y. Liu, P. Zuo, Z. Zhang, N. Lei, Y. Liu, Phthalocyanine-sensitized evolution of hydrogen and degradation of organic pollutants using polyoxometalate photocatalysts, *Env . Sci. Poll. Res*. (2020) 1-12.

[6] S. Roy, S. Sarkar, J. Pan, U.V. Waghmare, R. Dhanya, C. Narayana, S.C. Peter, Crystal Structure and Band Gap Engineering in Polyoxometalate-Based Inorganic–Organic Hybrids, *Inorg. Chem*., 55 (2016) 3364-3377.

[7] H. Mirhoseini, M. Taghdiri, Extractive oxidation desulfurization of sulfur-containing model fuel using hexamine-phosphotungstate hybrid as effective heterogeneous catalyst, *Fuel*, 167 (2016) 60-67.

[8] S. Mohammadghasemi-Samani, M. Taghdiri, Facile synthesis of hexamine–silicotungstic acid hybrid and its photocatalytic activity toward degradation of dyes, Int. J. Environ. Sci. Tech., 14 (2017) 2093-2108.

[9] J.M. Cameron, D.J. Wales, G.N. Newton, Shining a light on the photo-sensitisation of organic–inorganic hybrid polyoxometalates, *Dalton Trans.*, 47 (2018) 5120-5136.

[10] A. Enferadi-Kerenkan, T.-O. Do, S. Kaliaguine, Heterogeneous catalysis by tungsten-based heteropoly compounds, *Catal. Sci. Tech.* 8 (2018) 2257-2284.

[11] A. Baghernejad, M. Yaghoubi, Exergy analysis of an integrated solar combined cycle system, *Renewable Energy*, 35 (2010) 2157-2164.

[12] Z. Yao, G. Wang, Y. Shi, Y. Zhao, J. Jiang, Y. Zhang, H. Wang, One-step synthesis of nickel and cobalt phosphide nanomaterials via decomposition of hexamethylenetetramine-containing precursors, *Dalton Trans*., 44 (2015) 14122-14129.

[13] M. Agwara, P. Ndifon, M. Ndikontar, Physicochemecal studies of some hexamethylenetetramine metal (II) complexes, *Bulletin Chem. Soc. Ethiopia*, 18 (2004) 143-148.

[14] J. Joseph, R.C. Radhakrishnan, J.K. Johnson, S.P. Joy, J. Thomas, Ion-exchange mediated removal of cationic dye-stuffs from water using ammonium phosphomolybdate, *Mater. Chem. Phys*., 242 (2020) 122488.

[15] T. Zhaoyi, H. Zhaoya, Z. Dong, W. Xiaolin, Structural characterization of ammonium molybdophosphate with different amount of cesium adsorption, *J. Radioanal. Nucl. Chem.*, 299 (2014) 1165-1169.

[16] X.j. Zhou, Y.X. Ji, J.F. Cao, Z.F. Xin, Polyoxometalate encapsulated in metal-organic gel as an efficient catalyst for visible-light-driven dye degradation applications, *Appl. Organomet. Chem*., 32 (2018) e4206.

[17] X. Jia, L. Shen, M. Yao, Y. Liu, W. Yu, W. Guo, S. Ruan, Highly efficient low-bandgap polymer solar cells with solution-processed and annealing-free phosphomolybdic acid as hole-transport layers, *ACS Appl. Mater. Interfaces*, 7 (2015) 5367-5372.

[18] V.F. Hamidabadi, C. Momblona, D. Pérez-Del-Rey, A. Bahari, M. Sessolo, H.J. Bolink, Phosphomolybdic acid as an efficient hole injection material in perovskite optoelectronic devices, *Dalton Trans*., 48 (2019) 30-34.

[19] A. Prakash, A. Khadar, K. Patil, M. Hegde, Hexamethylenetetramine: a new fuel for solution combustion synthesis of complex

metal oxides, *J. Mater. Synth. Process*., 10 (2002) 135-141.
[20] S. Chouzier, T. Czeri, M. Roy-Auberger, C. Pichon, C. Geantet, M. Vrinat, P. Afanasiev, Decomposition of molybdate–hexamethylenetetramine complex: One single source route for different catalytic materials, *J. Solid State Chem*., 184 (2011) 2668-2677.
[21] P. Afanasiev, S. Chouzier, T. Czeri, G. Pilet, C. Pichon, M. Roy, M. Vrinat, Nickel and cobalt hexamethylentetramine complexes (NO3) 2Me (H2O) 6 (HMTA) 2· 4H2O (Me= Co2+, Ni2+): New molecular precursors for the preparation of metal dispersions, *Inorg. Chem*., 47 (2008) 2303-2311.
[22] G. Rao, W. Feng, J. Zhang, S. Wang, L. Chen, Z. Guo, W. Chen, Simulation approach to decomposition kinetics and thermal hazards of hexamethylenetetramine, *J. Therm. Anal. Calorim*., 135 (2019) 2447-2456.
[23] P. Afanasiev, Sponge-like silver obtained by decomposition of silver nitrate hexamethylenetetramine complex, *J. Solid State Chem*., 239 (2016) 69-74.
[24] S. Ilhan, C. Kahruman, I. Yusufoglu, Characterization of the thermal decomposition products of ammonium phosphomolybdate hydrate, *J. Anal. Appl. Pyrolysis*, 78 (2007) 363-370.
[25] C. Chen, W. Zhao, P. Lei, J. Zhao, N. Serpone, Photosensitized Degradation of Dyes in Polyoxometalate Solutions Versus TiO2 Dispersions under Visible-Light Irradiation: Mechanistic Implications, *Chem. Eur. J*., 10 (2004) 1956-1965.

هیبرید کردن فسفومولیبدیک اسید با هگزامین و هگزامین-نیکل به منظور افزایش فعالیت در تخریب نوری رنگ‌های آلی تحت تابش نورخورشید

مهدی تقدیری*[۱،۲]، فرزانه قانعی[۱]، مرضیه اردکانی[۱]، سید حسین بنی طبا[۱،۲]، حسین اعرابی اردکانی[۱]

۱. گروه شیمی، دانشگاه پیام نور، صندوق پستی۳۶۹۷-۱۹۳۹۵، تهران، ایران

۲. مرکز پژوهشی شیمی محیط‌زیست، دانشگاه پیام نور، اردکان، یزد، ایران

تاریخ دریافت: ۲۶ مرداد ۱۴۰۰ تاریخ پذیرش: ۳۰ شهریور ۱۴۰۰

چکیده

دو نوع هیبرید آلی جدید از فسفومولیبدیک اسید با استفاده از هگزامین و کمپلکس هگزامین-نیکل تهیه شد. اثرات هیبرید کردن هگزامین و هگزامین-نیکل روی فعالیت فتوکاتالیستی فسفومولیبدیک اسید مطالعه شد. برای شناسایی هیبریدها از طیف بینی زیر قرمز تبدیل فوریه، پراش اشعه‌ی ایکس، تجزیه گرما وزن سنجی و گرماسنجی روبشی تفاضلی استفاده شد. پهنای شکاف فسفومولیبدیک اسید، فسفومولیبدات-هگزامین و فسفومولیبدات-هگزامین-نیکل از طیف های بازتاب نفوذی و با استفاده از رسم نمودارهای تاک تعیین شد. خاصیت جذب و فتوکاتالیستی هیبریدها با بررسی رنگ‌زدایی محلول متیلن بلو، رودامین بی و مخلوط متیلن بلو- متیل اورانژ تحت نور خورشید مطالعه شد. نتایج حاصل نشان داد که هیبرید فسفومولیبدات-هگزامین-نیکل پهنای شکاف باریکتری داشته و بنابراین فعالیت فتوکاتالیستی آن در تخریب رنگ ها تحت تابش نورخورشید بیشتر است. مکانیسم تخریب نوری با افزودن بازدارنده ها مطالعه شد. حذف رنگ از طریق ترکیب جذب سطحی و سپس تخریب نوری به روش اکسایش توسط رادیکال ها صورت می گیرد.

واژه‌های کلیدی

فتوکاتالیست؛ پلی اکسومتالات؛ رنگ ها، پهنای شکاف ؛ هیبرید آلی-معدنی؛ نور خورشید.